Separation and Purification Technology 354 (2025) 129460

Contents lists available at ScienceDirect

Separation and Purification Technology

journal homepage: www.elsevier.com/locate/seppur

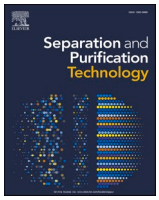

Donnan dialytic transport and biological removal of yttrium from multi-element solutions

Carina Coimbra [a], Svetlozar Velizarov [b,*], Rita Branco [a,*], Paula V. Morais [a], João G. Crespo [b,c]

[a] University of Coimbra, Centre for Mechanical Engineering, Materials and Processes, ARISE, Department of Life Sciences, Coimbra, Portugal
[b] LAQV-REQUIMTE, Department of Chemistry, NOVA School of Science and Technology, FCT NOVA, Universidade NOVA de Lisboa, 2829-516 Caparica, Portugal
[c] Instituto de Tecnologia Química e Biológica António Xavier, Universidade Nova de Lisboa, Av. da República, 2780-157 Oeiras, Portugal

ARTICLE INFO

Keywords:
Yttrium recovery
Critical raw materials
Cation-exchange membrane
Donnan dialysis
Yttrium-resistant bacteria

ABSTRACT

Yttrium (Y), classified among the rare earth elements (REEs), plays an important role in modern technologies, contributing to the increase in mineral extraction and processing activities. Consequently, this trend leads to an elevated release of economically significant but potentially dangerous elements into the environment. Acid mine drainage (AMD) is recognized as a concern due to the presence of hazardous elements, however, it simultaneously serves as a valuable secondary source of critical elements.

This study explores the recovery of Y(III) from multi-element solutions that simulate real AMD in terms of pH, the presence of various divalent cations, and sulfate. It investigates the recovery of Y(III) from multi-element solutions using a two-stage approach: cation exchange membrane (CEM) for Donnan dialytic Y(III) transport followed by biological treatment for Y recovery. The efficiency of Y(III) transport across the acid-resistant CEM, Fumasep FKS-PEP-130, reached 68.6 %, even in the presence of accompanying cations. The addition of strain J19, highly resistant to Y, led to approximately 89 % removal of Y(III) from the feed compartment.

The proposed CEM transport/biological treatment concept offers the first efficient Y(III) recovery approach. This method will benefit future assays with real-field AMD, as it minimizes waste generation while effectively separating metals from sulfate, thereby reducing environmental impact.

1. Introduction

Yttrium (Y) belongs to the rare earth elements (REEs) group [1], and like other REEs, it does not occur naturally as a free element. They are present in a wide range of mineral types, including halides, carbonates, oxides, phosphates and silicates [2], and have a predominant preferred electronic configuration with dominant oxidation states of + 3, Y(III) [3–5]. Yttrium has gathered increasing attention due to its valuable applications in several fields, including manufacturing high-tech, military and biomedical products. Consequently, Y is considered strategically important and is included in the European list of critical raw materials [6]. It is crucial to find alternative REE sources to meet the predicted growing demand that could exceed the world supply. The use of primary REE resources, as well as REEs from waste streams, will be essential to meet this demand. In this context, exploring and identifying secondary REE resources and developing novel, cost-effective, and sustainable techniques is necessary. Recent studies have shown the viability of acid mine drainage (AMD) as a strategic secondary source of REEs [3,7–10].

The occurrence of REEs, more specifically Y, in natural water sources is a consequence of environmental pollution caused by the extraction and processing of mineral resources [11]. Due to their high chemical and thermal stability, REE minerals can only be dissolved by adding concentrated sulfuric acid or sodium hydroxide at high temperatures (around 300 °C). This chemical action with sulfuric acid, resulting from mining activity, increases the dissolution capacity of REEs, thereby leading to the presence of many sources of AMD [12,13]. AMD treatment is of great concern worldwide due to the long-lasting nature of AMD, which can persist for decades or even centuries. When left untreated, AMD can generate leachate that commonly releases large amounts of metal(oid)s, sulfate (up to 20 g/L), and acidity into streams and groundwater [14,15]. Typically, AMD is characterized by a low pH ranging from 2 to 4 and by high concentrations of dissolved valuable compounds containing iron (Fe), aluminium (Al), zinc (Zn), copper (Cu), arsenic (As), antimony (Sb) and selenium (Se) [3,10,14,15]. In addition to the mentioned ones, AMD also contains high concentrations of

* Corresponding authors.
E-mail addresses: s.velizarov@fct.unl.pt (S. Velizarov), rbranco@uc.pt (R. Branco).

https://doi.org/10.1016/j.seppur.2024.129460
Received 14 June 2024; Received in revised form 27 August 2024; Accepted 30 August 2024
Available online 1 September 2024

dissolved REEs above 1 mg/L or with an average of 2.25 mg/L as the studies from the Iberian Pyritic Belt [7,16].

The traditional approach to treating AMDs is via neutralization (using lime ($Ca(OH)_2$), limestone ($CaCO_3$), among others), which causes precipitation of sulfate and metals. This process generates large amounts of toxic sludge that are environmentally harmful, and the handling, treatment, and disposal of this sludge are expensive and labor-intensive [10,14,15]. Alternative treatment methods, such as ion-exchange, membrane crystallization, and sulfide precipitation, each have their unique advantages and disadvantages. Ion-exchange provides high selectivity and purity but requires complex resin regeneration [17,18]. Membrane crystallization effectively recovers high-purity materials but is energy-intensive [19]. Sulfide precipitation is simple and cost-effective but generates waste sludge [20,21]. In contrast, membrane processes using Donnan dialysis, offer cost-effective and scalable solutions without needing an electrical field, offering advantages over the methods mentioned above. Donnan dialysis combines good selectivity with low energy requirements, making it an attractive option compared to conventional AMD treatment processes [22–24]. Donnan dialysis uses an ion exchange membrane (IEM) to separate and concentrate ions of interest from a target aqueous solution, driven by an electrochemical potential. The IEM is impermeable to co-ions, while counter-ions are transported to a receiving (stripping) compartment [25], where "driving" counter-ions are added at a higher molar concentration than that of the target ions in the feed. The conceptual sketch of Donnan dialysis using a cation-exchange membrane is presented in the supplementary material as Fig. S1. This low-energy method has been used to remove contaminants (e.g., arsenate, nitrate, fluoride, perchlorate) and recover valuable compounds (e.g., gold, silver, Cu, chromium, lithium, ammonia and phosphorus) from industrial waste streams [22–24,26–32]. Research on removing Y(III) from aqueous solutions by Donnan dialysis reported is very scarce. However, Matsuyama et al. [26] demonstrated that Y(III) ions can be effectively transported across a Neosepta CM-1 membrane in a synthetic solution using H^+ or K^+ as the "driving" counter-ion in the stripping solution. This finding is particularly valuable for cation exchange membranes (CEMs) with lower stability in highly acidic (low pH) conditions. Another study demonstrated that Y(III) ions, when using a Selemion CMV membrane, have a much lower self-diffusion coefficient than H^+ due to their larger size and trivalent state, significantly hindering their transport [33].

Several authors [34–38] have studied the combined use of biological treatments and ion exchange membrane processes, particularly in ion exchange membrane bioreactors for drinking water treatment. Biological treatment is highlighted as the most cost-effective and environmentally friendly method for metal removal from wastewater. Metal recovery can be achieved through bioaccumulation, which involves cellular metabolic activities, or through biosorption, which involves the presence of specific functional groups within cellular structures capable of forming chemical bonds with metals [38–43]. In biological treatments, bacteria are optimal biosorbents due to their high adsorption capacity, rapid growth cycle, and adaptability [43,44]. They can concentrate, remove, and recover metals from polluted environments and survive in high concentrations of metal pollutants [45,46]. Biomineralization, another biological process, involves the deposition of inorganic minerals within or outside the cells as a mechanism of bacterial resistance to metal toxicity [47]. This phenomenon is supported by various studies demonstrating biomineralization through metal-complex deposition [47–50].

The primary limitations of existing treatment technologies include the risk of secondary contamination from microbial cells, nutrients, and metabolic by-products in biological processes. In this study, we suggest a potential solution to overcome these issues by introducing the concept of integrated CEM transport with biological treatment. With this proposal, this study aims to develop an initial system to recover Y(III) from multi-element solutions that simulate real AMD in terms of pH, the presence of various divalent cations, and sulfate. The study initially explores and compares the impact of using HCl, NaCl, or a combination of both in the receiver solution to optimize the efficiency of Y(III) transport. Secondly, the study also investigates the influence of defined divalent cations in a multi-element solution, along with sulfate, on the efficiency of Y(III) transport. Our proposed concept is divided into two distinct stages. The first stage involves the transport of Y(III) across the membrane. In the second stage, we evaluate the addition of a culture of the bacterial strain *Mesorhizobium qingshengii* J19, known for its high tolerance to Y and its ability to immobilize it, to the receiver solution. Our proposed concept presents a promising environmental bioremediation strategy since it will offer benefits in future assays with aqueous secondary sources such as real-field AMD by reducing waste generation and efficiently isolating metals from sulfate, thus reducing environmental impact.

Table 1
Main characteristics of the Fumasep® FKS-PET-130 membrane, according to the manufacturer (Fumatech BWT GmbH, Bietigheim-Bissingen, Germany).

Appearance/color	light brown
Reinforcement	PET
Counter-ion	H^+
pH stability range at 25 °C	0–8
Area resistance in 0.5 M NaCl at 25 °C	$<4\ \Omega.cm^2$
Thickness	120–150 μ m

2. Material and methods

2.1. Reagents, membrane and bacterial strain growth conditions

All reagents used, such as $YCl_3{\cdot}6H_2O$ (Sigma-Aldrich), K_2HPO_4 (Ensure), $MgSO_4{\cdot}7H_2O$ (LabChem), NaCl (NZYTech), $CaSO_4{\cdot}2H_2O$ (Merck), $MnCl_2{\cdot}4H_2O$ (Acros Organics), $NaSO_4$ (PanReac AppliChem) and $NaNO_3$ (Merck) were of analytical grade. An aqueous 0.5 M $YCl_3{\cdot}6H_2O$ was prepared as a stock solution and sterilized by filtration through a filter 0.2 μ m to provide Y(III) in its trivalent cationic form, Y^{3+} If it were present as YSO_4^+, the affinity of the CEM would be expected to be reduced due to the monovalent nature of the cation. All solutions were freshly prepared with deionized water (conductivity $\leq$ 1 μS/cm). The desired pH values of the receiver and feed solutions were adjusted using 37 % HCl (Fluka) and 0.1 M H_2SO_4 (Fluka), respectively.

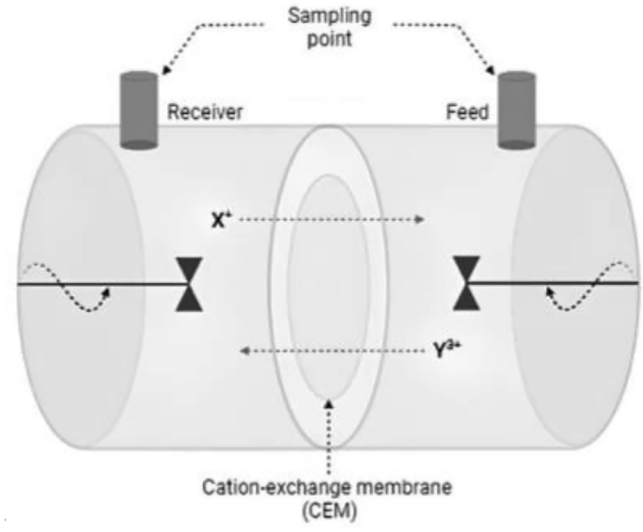

Fig. 1. A schematic representation of the dialysis cell used in this work. Y^{3+} cation, transported through the CEM from the feed compartment is shown. In the receiver, X^+ represents the "driving" Na^+ or H^+ counter-ions used in the present study. The dashed spiral arrows indicate the movement of the magnetic stirrer in each compartment, while the straight dashed arrows represent the exchange process of cations and anions through the CEM.

Table 2
Experimental conditions of the Donnan dialysis assays performed in the present study without the presence of other co-cations in the feed solution, except for Y.

	Solutions		Driving counter-ions	pH	
Assay	**Receiver**	**Feed**	**Receiver**	**Receiver**	**Feed**
1st	1.72 mM K_2HPO_4 0.1 mM $MgSO_4$ 0.5 M NaCl	0.5 mM $YCl_3{\cdot}6H_2O$	Na^+, K^+, Mg^{2+}	7.37	5.55
2nd	1.72 mM K_2HPO_4 0.1 mM $MgSO_4$ 0.5 M NaCl	5 mM $YCl_3{\cdot}6H_2O$	Na^+, K^+, Mg^{2+}, H^+	3[a]	5.02
3rd	1.72 mM K_2HPO_4 0.1 mM $MgSO_4$ 0.5 M NaCl	5 mM $YCl_3{\cdot}6H_2O$	Na^+, K^+, Mg^{2+}, H^+	1[a]	4.19
4th	1.72 mM K_2HPO_4 0.1 mM $MgSO_4$ 0.5 M NaCl	5 mM $YCl_3{\cdot}6H_2O$	Na^+, K^+, Mg^{2+}, H^+	0.8[a]	3[b]
5th	1.72 mM K_2HPO_4 0.1 mM $MgSO_4$	5 mM $YCl_3{\cdot}6H_2O$	K^+, Mg^{2+}, H^+	0.8[a]	3[b]
6th	1.72 mM K_2HPO_4 0.1 mM $MgSO_4$ 0.26 M NaCl	5 mM $YCl_3{\cdot}6H_2O$	Na^+, K^+, Mg^{2+}, H^+	0.8[a]	3[b]

[a] pH adjusted with 37 % HCl; [b] pH adjusted with 0.1 M H_2SO_4.

A commercial CEM, Fumasep® FKS-PET-130 (FuMA-Tech), was used because of its high stability in an acidic environment. The membrane is polyester(PET)-reinforced with low electric resistance, and high mechanical stability. Since the membrane is delivered in a dry form, a pretreatment was done: the membrane was first immersed in a 0.5 M NaCl aqueous solution for a minimal time of 48 h so that it could be converted into the Na^+ form. Afterwards, it was thoroughly rinsed with distilled water. The main membrane properties are listed in Table 1.

The bacterial strain *M. qingshengii* J19, an Alphaproteobacterium belonging to the University of Coimbra Bacteria Culture Collection (UCCCB) and isolated from the surface of test galleries at the Jales mine, was grown aerobically at 25 °C in Reasoner's 2A (R2Ab) liquid medium (Himedia). The medium contained per liter: 0.5 g yeast extract, 0.5 g proteose peptone, 0.5 g casein, 0.5 g glucose, 0.5 g soluble starch, 0.3 g K_2HPO_4, 0.024 g $MgSO_4$ and 0.3 g sodium pyruvate. To determine the colony-forming units (CFUs) of strain J19 when grown in the receiver solution, R2A solid medium was used, which is R2Ab liquid medium supplemented with 1.5 % agar.

2.2. Donnan dialysis experiments

The assays were carried out in a two-compartment membrane cell (190 mL each) equipped with a circular window for the membrane (area of 11.3 cm^2), as schematically shown in Fig. 1. Each compartment was fitted with a magnetic stirrer to avoid possible concentration polarization effects at the membrane surface. The membrane was fixed between the two half-cells of the system, and the receiver and feed solutions used in a given experiment were placed in the respective compartments of the cell for membrane pre-equilibration. The working solutions used in the assays were kept in the compartments for 2 h (without stirring) and then removed. Fresh solutions were then added, and the assays were initiated by starting the stirring (700 rpm). All assays were performed at an air-controlled room temperature of 23°C.

Table 3
Multi-element solution composition used in the feed compartment (the pH of the final solution was adjusted to 3 with 0.1 M H_2SO_4).

Salt	**Ion**	**Concentration (mM)**
$CaSO_4{\cdot}2H_2O$	Calcium, Ca^{2+} Sulfate, SO_4^{2-}	1.5
$MgSO_4{\cdot}7H_2O$	Magnesium, Mg^{2+} Sulfate, SO_4^{2-}	10
$MnCl_2{\cdot}4H_2O$	Manganese, Mn^{2+} Chloride, Cl^-	2.5
Na_2SO_4	Sulfate, SO_4^{2-} Sodium, Na^+	60
NaCl	Chloride, Cl^- Sodium, Na^+	90
$NaNO_3$	Nitrate, NO_3^- Sodium, Na^+	16
$YCl_3{\cdot}6H_2O$	Yttrium, Y^{3+} Chloride, Cl^-	0.2 or 0.4

At pre-defined time intervals, 2 mL aliquots were collected from both receiver and feed compartments to measure pH (SensION™ pH3) and conductivity (SensION™ EC7). The assays were conducted over 72 h, monitoring the transient change in Y(III) concentrations in both compartments using the Arsenazo III colorimetric method. The procedure described by Hogendoorn et al. [29] was followed, with appropriate volume adjustments to achieve a final reaction volume of 2 mL. Quantification was performed by mixing 1 mL of citric acid/phosphate buffer (pH 2.8), 980 µL of sample and 20 µL of 1 mM Arsenazo III, then analyzing the samples spectrophotometrically at 655 nm. Yttrium concentrations from 0.025 to 0.5 mM were used to generate a standard calibration curve. Furthermore, recent work showed no significant change in Y quantification over time when abiotic controls with increasing Y concentrations in growth medium (also including K_2HPO_4 as in the receiver solution of the present work) were filtered with a 0.1 µm filter before measurement. This step was essential, as colloidal Y(III) precipitates are difficult to pellet through centrifugation [52].

Six sets of assays were performed and are presented in Table 2 in sequential order. The first assay started without changing the naturally obtained pH of the solutions to evaluate the degree of Y(III) recovery under these conditions. In the next two assays, the Y(III) concentration in the feed solution was increased 10-fold, while the pH of the receiver solution was reduced. This was done to explore the effect of higher H^+ ion concentrations and lower pH on the Y(III) recovery rate. The fourth assay used a feed solution with a pH closer to that encountered in AMD, reducing the pH to 3. To verify whether and how Na^+ ions affected transport across the membrane, the last two sets of assays were designed and carried out, in which NaCl was either not added to the receiver solutions or its content decreased to almost half of its initial concentration. The membrane was regenerated between each set of assays by placing it in a 0.5 M NaCl solution (renewed several times) and rinsing it with distilled water.

2.3. Multi-element solution design

The multi-element solution used in this study was adapted from the work of Siew et al. [15], based on the average composition of six different real AMD water samples. The composition of the multi-element feed solution is presented in Table 3. Yttrium was added to the multi-element solution, testing two different concentrations: 0.2 and 0.4 mM.

The assay was performed at room temperature in a two-compartment membrane cell. Samples were collected from both receiver and feed compartments over 96 h. The pH and conductivity were also measured. The Y concentrations in both compartments were measured by inductively coupled plasma mass spectrometry (ICP-MS) at the Trace Analysis and Imaging Laboratory of the University of Coimbra (TAIL-UC). Magnesium (Mg), manganese (Mn), sulfur (S), sodium (Na), and potassium (K) were also measured using ICP-MS. The results were presented as a

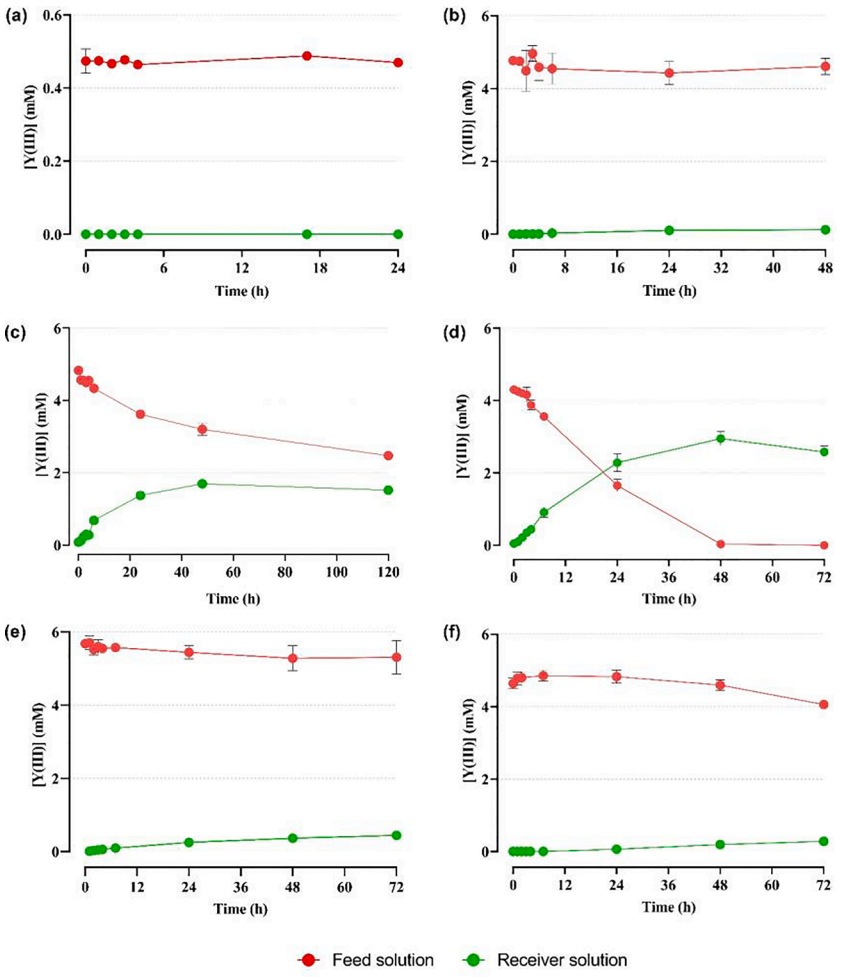

Fig. 2. Concentration of Y(III) measured in both receiver (green line) and feed (red line) solutions over time for the six sets of assays. **(a)** 1st assay: 0.5 M of NaCl in the receiver solution and 0.5 mM of Y(III) in the feed solution, **(b)** 2nd assay: 0.5 M of NaCl and pH 3 in the receiver solution, and 5 mM of Y(III) in the feed solution, **(c)** 3rd assay: 0.5 M of NaCl and pH 1 in the receiver solution, and 5 mM of Y(III) in the feed solution, **(d)** 4th assay: 0.5 M of NaCl and pH 0.8 in the receiver solution, and 5 mM of Y(III) and pH 3 in the feed solution, **(e)** 5th assay: pH 0.8 (without NaCl) in the receiver solution, and 5 mM of Y(III) and pH 3 in the feed solution, **(f)** 6th assay: 0.26 M of NaCl and pH 0.8 in the receiver solution, and 5 mM of Y(III) and pH 3 in the feed solution. Means ± standard deviations – error bars – were calculated from two independent experiments. (For interpretation of the references to colour in this figure legend, the reader is referred to the web version of this article.)

ratio, where concentrations over time were normalized to the initial concentration in the feed.

2.4. Y(III) removal using strain m. Qingshengii J19 from the receiver compartment

The Donnan dialysis cell was sterilized in two steps to ensure maximum sterility for bacterial growth. First, the system and all the connecting tubing, sampling ports and O-rings were immersed in 70 % ethanol (v/v) for 48 h. Afterwards, it was dried and sterilized by UV-A light irradiation for at least 1 h (or until completely dry).

The 1st stage of this assay involved the transport of Y(III) from the feed to the receiver solution compartment across the CEM. This transport occurred for 48 h, using the compositions of the receiver (4th assay described in Table 2) and multi-element feed solutions (as mentioned in Section 2.3), both autoclaved at 121 °C for 20 min (Y(III) added separately). The concentration of Y(III) used in this step was 0.4 mM. Afterwards, and before starting the 2nd stage, half of the receiver solution was discarded and the same volume of 2x concentrated R2Ab medium was added. The pH was adjusted to approximately 7 with 1 M NaOH. Once the solution reached a neutral pH, strain J19 was added to the receiver compartment, starting with an optical density at 600 nm (OD_{600}) of 0.06. The assay was performed for 48 h.

The assays were performed at room temperature. Samples were collected for Y measurement by ICP-MS at several time points: at t0 and t48 for the 1st stage in both compartments, and at t0, t24, and t48 for the 2nd stage in the receiver compartment. Bacterial cells were collected by centrifugation at maximum speed (17,000 g) for 15 min, then washed with a phosphate-buffered saline solution (PBS), containing per liter: 8 g NaCl, 0.2 g KCl, 1.44 g Na_2HPO_4, 0.24 g KH_2PO_4 and pH 7.4, and lysed by an acidic lysis procedure [50]. The supernatants, resulting from the bacterial cell lysis step, were measured by ICP-MS, while the cellular pellets were neutralized with 0.5 M NaOH and then used to quantify total protein using the Bradford method [51]. The Y values obtained were normalized by the total protein mass. Moreover, in the 2nd stage, serial 10-fold dilutions in sterile 0.85 % NaCl (w/v) were performed, and 100 µL were spread on R2A agar plates to determine the CFUs as a control of bacterial growth during the assay. The plates were incubated at 25 ℃ until colonies were visualized.

2.5. Scanning electron microscopy with coupled energy-dispersive X-ray spectroscopy (SEM-EDS)

After Y(III) transport from the 1st stage assay, the Fumasep® FKS-

PET-130 membrane that had been in contact with the feed solution was observed by SEM-EDS in backscattered electron mode (BSE). The membrane was first washed with sterile Milli-Q water, dried, to ensure accurate and reliable results, and then stored until analysis. This was done to ensure only the Y bound to the membrane was analyzed, avoiding interference from the feed solution. SEM micrographs were obtained on a FEI Quanta 400 FEG ESEM, and EDS analysis was accomplished using an Oxford INCA Energy 350 equipped with the SAMX IDEFIX software, with an accelerating voltage of 15 kV and a beam current of 20 nÅ.

2.6. Maximum Y(III) removal

The assay was conducted following the procedure outlined in Section 2.4, with the only difference being that it was performed in repeated batch process mode. Briefly, the system operated in three batches as follows: batch 1 involved starting the assay with new solutions and performing the 1st and 2nd stages; batch 2 involved renewing the receiver solution while keeping the same feed solution, and performing the 1st and 2nd stages; and batch 3 involved a second renewal of the receiver solution, with the same feed solution, and again performing the 1st and 2nd stages. The initial Y(III) concentration in the multi-element feed solution was 0.4 mM, and the membrane remained in the system between both compartments throughout the assay. Aliquots were taken for Y measurement by ICP-MS at t0 and t48 for all 1st stages and at t0, t24 and t48 for all 2nd stages.

2.7. Analytical method: Colorimetric quantification of yttrium

In all assays from Section 2.2, to monitor the transient change in Y (III) concentrations in both the receiver and feed compartments, samples were periodically measured using Arsenazo III (1,8-dihydroxynaphthalene3,6-disulphonic acid-2,7-bisSTA(azo2)-phenylarsonic acid) (Sigma-Aldrich) colorimetric method, following the procedure described in the literature [52]. Briefly, quantification was performed by mixing 1 mL of citric acid/phosphate buffer (pH 2.8), 980 μL of sample, and 20 μL of 1 mM Arsenazo III. Samples were quantified by spectrophotometry at 655 nm and Y concentrations from 0.025 to 0.5 mM were used to generate a standard curve.

2.8. Calculations

The obtained data were compared in terms of Y(III) recovery (i.e., the amount of Y(III) present in the receiver compartment) and the yield of Y(III) accumulation by the bacterial strain J19 from the receiver solution. The percentage of Y(III) transported to the receiver compartment over time was calculated through the following equation:

$$\text{Y(III) recovery (\%)} = \frac{[\text{Y(III)}], \text{receiver(tx)}}{[\text{Y(III)}], \text{feed(t0)}} \times 100 \quad (1)$$

where [Y(III)],receiver(tx) and [Y(III)],feed(t0) represent the Y(III) concentrations at an elapsed time, tx and time 0 in the receiver and feed compartments, respectively.

The Y accumulation yield (%) by strain J19 was calculated using the following equation:

$$Yaccumulationyield(\%) = \left(\frac{W, receiver(tx)}{W, receiver(t48)}\right) \times 100 \quad (2)$$

where W,receiver(tx) represents the Y weight (mg) accumulated by strain J19 at an elapsed time tx in the receiver compartment, while W, receiver(t48) denotes the weight (mg) measured at time 48 h in the receiver compartment during the first stage, i.e., before bacterial inoculation.

Table 4
Summary of Y(III) recoveries obtained in the assays performed (Means ± standard deviations were calculated from two independent experiments).

Assay	Assay duration (h)	Y(III) recovery (%), Eq. (1)
1st	24	0 ± 0.002
2nd	48	2.7 ± 0.008
3rd	120	35.0 ± 0.12
4th	72	68.6 ± 0.19
5th	72	7.8 ± 0.003
6th	72	6.0 ± 0.02

2.9. Statistical analysis

Each result is shown as the mean value of two independent assays (the number of independent assays is indicated in the caption of each figure) ± the standard deviation. Statistical analysis was performed using GraphPad Prism 9 for Windows, using Two-way ANOVA and Ordinary one-way ANOVA followed by Šídák's and Tukey's, and Dunnetts's multiple comparisons tests, respectively. A difference was considered statistically significant if p-value < 0.05.

3. Results and Discussion

3.1. Y(III) transport by Donnan dialysis

The Y(III) time concentration profiles in the receiver and feed compartments are presented in Fig. 2 for the six assays performed. The Y(III) transport from the feed to the receiver solution was not significantly affected by a 10-fold increase in the initial Y(III) concentration (from 0.5 to 5 mM) in the feed solution (Fig. 2a and 2b, respectively), showing in both cases a very low removal yield of Y(III) from the feed solution of 0.9 and 3.3 %, respectively. As is well-known, trivalent cations have much higher affinities than monovalent ones to strong acidic cation exchangers with sulfonic functional groups [53]. Therefore, decreasing the pH to 3 and 1 (Fig. 2b and 2c, respectively) in the receiver solution (i.e., more H^+ ions present) did not provide enough "driving" H^+ ions to ensure a significant counter-transport of Y(III) from the feed to the receiver compartment. Thus, the receiver solution pH was further decreased to 0.8 (Fig. 2d). This improved the efficiency of the cationic exchange of Y^{3+} ions, reaching a recovery of Y(III) in the receiver compartment of 68.6 % (Table 4). The results are consistent with previous findings, which showed that the highest recovery of REE using a strong acid sulfonic resin occurred at pH levels between 0.5 and 2 [10]. Still, not all Y(III) was quantitatively transported to the receiver due to its strong affinity for the membrane functional groups.

Given these observations, additional assays were performed to evaluate the possible contribution of "driving" Na^+ counter-ions (present in the form of NaCl) to the degree of Y(III) recovery in the receiver compartment. Maintaining pH levels at 0.8 and 3 in the receiver and feed solutions, respectively, the 5th and 6th assays were performed without NaCl and with half the concentration of NaCl (0.26 M) in the receiver solution compared to the first four assays. As shown in Fig. 2e and 2f, respectively, the recovery of Y(III) was influenced by the presence of Na^+ ions in the receiver. In assays without salt and with half the concentration of salt, Y(III) recovery was only 7.8 and 6 %, respectively (5th and 6th assay in Table 4), compared to the 68.6 % obtained in the 4th assay, where the highest concentration of NaCl (0.5 M) at the lowest pH (0.8) was used as the receiver solution. The Y(III) recovery in the receiver was almost one order of magnitude lower than that found in the 4th assay, i.e., recovering around 10-fold less Y(III) in the receiver compartment. These results indicate that the presence of Na^+ ions in the receiver compartment slightly contributes to increasing the recovery of Y^{3+} ions, while the presence of a high concentration of H^+ ions (pH<1) is essential for ensuring efficient Y^{3+} ions transport. As mentioned, the affinity towards cations increases with the increasing cation charge. However, in the case of different cations with the same charge, such as

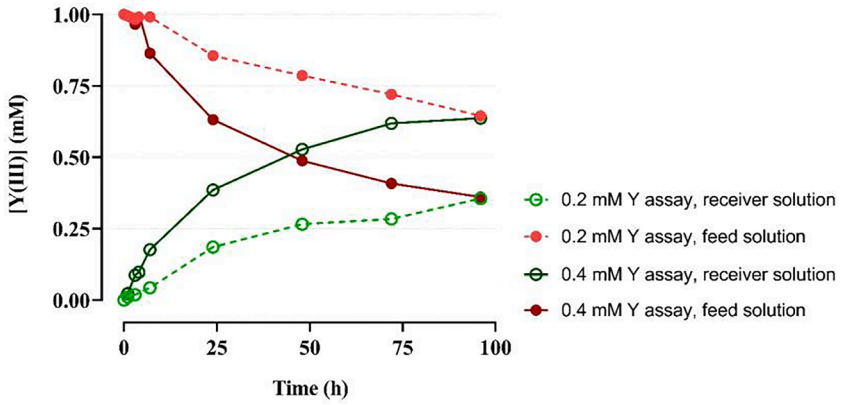

Fig. 3. Concentration of Y(III) measured in both receiver and feed solutions over 96 h of the assay 0.2 mM (light green and light red, respectively) and 0.4 mM (dark green and dark red, respectively) of Y(III) were added to the muti-element feed solution. Means ± standard deviations – error bars – were calculated from two independent experiments. (For interpretation of the references to colour in this figure legend, the reader is referred to the web version of this article.)

H^+ and Na^+ ions, we observe that cation exchangers have a lower affinity for Na^+ ions compared to H^+ ions. Due to the highest mobility of protons compared to all other possible "driving" counter-ions, such as Na^+ ions, the strongly acidic environment enhances the affinity of Y^{3+} ions for the resin's functional groups, facilitating their transport across the membrane. Since no significant change in Y quantification was observed over time with abiotic controls filtered through a 0.1 μm filter to remove colloidal precipitates, this suggests that phosphate present in the growth medium did not interfere with metal precipitation, indicating any interference between these two elements when both are present in the present study's receiver solution.

Comparing the pH profiles of all the assays (Fig. S2 in Supplementary Information), the pH remained relatively stable in both receiver and feed compartments over time, except in the 3rd and 4th assays. When HCl was used to lower the pH of the receiver solution to 3 and 0.8 (Fig. S2c and S2d, respectively), the migration of H^+ ions caused a decrease in the feed's pH and a slight increase in the receiver's pH. The conductivity profiles (Fig. S2 in Supplementary Information) showed minimal or negligible decreases in both compartments, except in the 2nd and 4th assays. It is notable that while the conductivity decreased in the

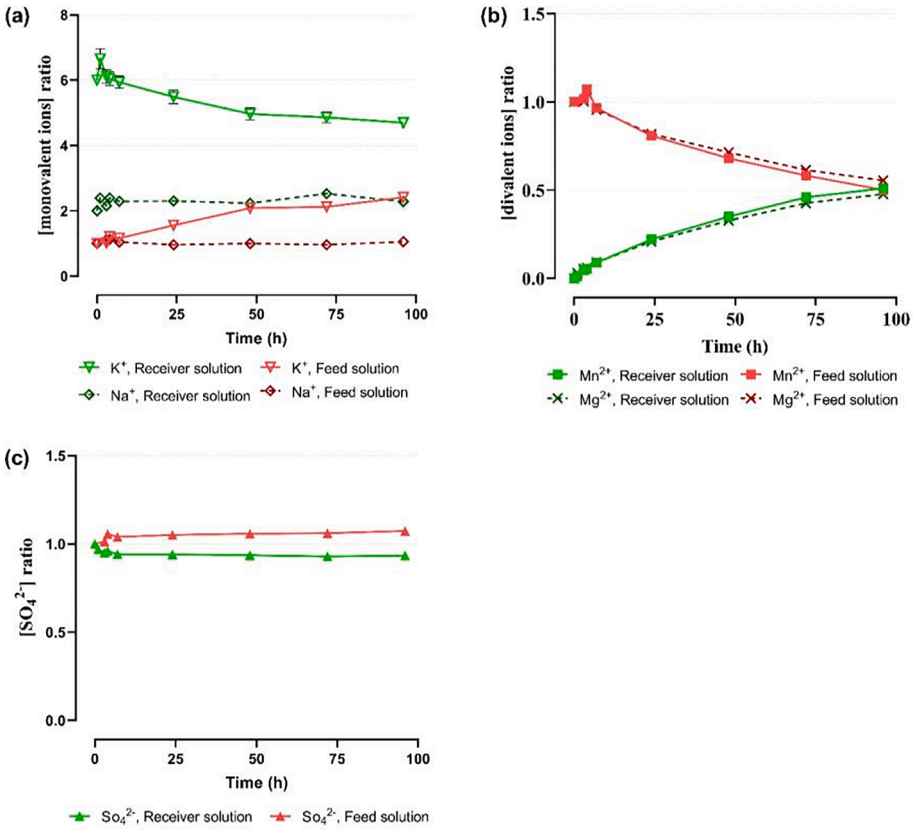

Fig. 4. Ratios of the concentration of the monovalent counter-ions potassium (K+: potassium, inverted triangle) and sodium (Na+: sodium, rhombus) **(a)**, divalent counter-ions manganese (Mn2+: manganese, square) and magnesium (Mg2+: magnesium, cross) **(b)** and co-ion sulfate (SO42-, triangle) **(c)** measured in both receiver (green line) and feed (red line) solutions over 96 h of the assay when 0.4 mM of Y(III) were added to the multi-element feed solution. The concentrations over time were normalized to the initial concentration in the feed, expressed as a ratio. Means ± standard deviations – error bars – were calculated from two independent experiments. (For interpretation of the references to colour in this figure legend, the reader is referred to the web version of this article.)

receiver compartment, it remained constant in the feed compartment.

In sum, the most promising results for Y(III) transport were obtained when using 0.5 M NaCl at pH 0.8 in the receiver compartment, where both Na^+ and H^+ served as "driving" counter-ions.

3.2. Y(III) transport using a multi-element feed solution

Given the complexity of real AMD samples, it is important to evaluate the Y(III) transport in such solutions, referred to as multi-element solutions, with a composition presented in Table 3. The concentration of Y(III) present in both receiver and feed compartments of the assays performed with the multi-element solution is shown in Fig. 3.

Two increasing concentrations of Y(III) were added to the multi-element feed solution, 0.2 and 0.4 mM, resulting in the highest Y(III) recovery in the receiver solution (Fig. S3 and 4, respectively). The results showed that the recovery of Y(III) in the receiver solution increased with higher Y(III) concentrations, with the fastest recovery observed at the highest concentration tested, 0.4 mM. In the first 7 h, a Y(III) recovery of 4.3 ± 0.012 and 17.7 ± 0.09 % was achieved for the assays performed with 0.2 and 0.4 mM Y(III), respectively. After 96 h, the Y(III) recovery had further increased to 35.6 ± 0.15 and 63.7 ± 0.31 %, for the respective concentrations. Although conducted under different conditions, a reported study using acid mine waters from an abandoned mine at La Poderosa in the Odiel river basin (Huelva, Spain) showed a removal of Y(III) of 9.3 %, which is 6.9 times lower than the values obtained in our study with a multi-element solution [3].

The concentrations of other cations present in the multi-element solution, namely monovalent ions K^+ and Na^+, and divalent ions Mg^{2+} and Mn^{2+}, were also measured and are presented in Fig. 4a and 4b. Na^+ ions were not transported from the feed to the receiver, due to their presence as a "driving" counter-ion in the receiver compartment (Fig. 4a). Over time, Mg^{2+} and Mn^{2+} ions were transported across the membrane from the feed to the receiver solution, reaching maximum recoveries of 47.8 ± 0.14 % for $Mg^{2+}$and 51 ± 0.03 % for Mn^{2+} after 96 h (Fig. 4b). Thus, both elements were recovered approximately up to 1.3-fold less when compared to the recovery of Y(III) in the same compartment. Lowering the concentration of Y(III) to 0.2 mM resulted in Mg^{2+} recoveries of 28.9 ± 0.35 % and Mn^{2+} recoveries of 34.1 ± 0.08 % (Fig. S3b in Supplementary Information). In conclusion, the recovery of both ions, Mg^{2+} and Mn^{2+}, increased with rising concentrations of Y (III), from 0.2 to 0.4 mM.

These findings confirm the absence of significant competition with co-cations, such as Mn^{2+} and Mg^{2+}, in the presence of other divalent cations. Even when the initial concentration of Mg^{2+} in the feed solution was 100 times higher than that in the receiver solution (10 and 0.1 mM, respectively), it did not affect the transport of Y^{3+}. This indicates that high amounts of Mg^{2+} do not interfere with the transport of Y^{3+}, ensuring efficient transport regardless of Mg^{2+} concentration differences. This can be explained by the fundamental principle of cation exchange, where the high affinity of a trivalent cation compensates for the presence of a divalent ion, even at higher concentrations [53]. Fig. 4b also shows that the temporal dynamics and the relative amounts transported from the feed to the receiver solutions are similar for both mentioned cations. Although conducted under different conditions, the reported study using AMD from an abandoned mine showed a removal of Mg and Mn of 9.5 and 4.6 %, respectively [3]. These values are 4.7 and 10.9 times lower than those observed in the current study performed with the multi-element solution. In addition to the mentioned counter-ions, the co-ion sulfate (SO_4^{2-}) was also followed in both compartments, and the results are presented in Fig. 4c. As expected, the SO_4^{2-} ion was not transported since it is a co-ion with the same charge as the functional group of the ion exchange membrane under study. This confirms its efficient Donnan co-ion exclusion. The same result was obtained with 0.2 mM Y(III) (Fig. S3c in Supplementary Information). As mentioned earlier, many real AMD contain valuable metals dissolved in the acidic water, along with sulfate [3,10,14,15]. For instance, one study reported very high concentrations of Fe (822.029 mg/L), Mn (199.673 mg/L), Cu (10.704 mg/L), Zn (8.328 mg/L), and Pb (1.877 mg/L) in a AMD with sulfate concentrations reaching 4455.87 mg/L. Additionally, lower concentrations of other significant metals, such as Ni, Cd and As (<1 mg/L) were detected [54]. All these concentrations far exceeded the established standards for these metals. Sulfate concentrations in AMD often range from 500 and 3000 mg/L, significantly surpassing the maximum recommended limit of 250 mg/L for drinking water [55]. Metals in AMD are usually present at toxic levels, but they generally occur at lower concentrations than sulfates. The high sulfate levels, which can vary widely depending on the specific mine site and the minerals present, represent a significant environmental challenge. Applying CEM for separating sulfate from cations in AMD waters is crucial for environmental remediation, allowing the potential to recover the cationic metals in subsequent processes. Remarkable results were obtained in this study using the Fumasep FKS-PEP-130 membrane, effectively separating sulfate from Mg^{2+}, Mn^{2+}, and Y^{3+} cations. High concentrations of sulphate interfere negatively with bacterial growth and, consequently, with the Y removal or immobilization bioprocess. Separating anions like sulfate from cations in the solution is a crucial step that significantly enhances the efficiency of subsequent cation removal, particularly in the second stage of the process when a bacterial culture is introduced. By removing sulfate, the solution is less complex, reducing potential interference and competitive interactions between anions and cations. Consequently, the bacterial culture can operate more efficiently, facilitating the desired cation extraction without the hindrance of competing anions. The pH and conductivity time profiles obtained are presented in Fig. S4 in Supplementary Information. Comparing the pH profiles for each assay, it can be observed that the pH in the feed compartment slightly decreased from 3 to 2 at the highest Y (III) concentration used, whereas the pH in the receiver compartment remained constant over time. Regarding conductivity, there were minimal or negligible fluctuations in both compartments when 0.2 mM of Y (III) was used in the multi-element feed solution. However, increasing the concentration of Y(III) to 0.4 mM caused the conductivity to drop much more in the receiver compartment compared to its increase in the feed compartment.

The negligible competing effect of other co-cations present in the multi-element feed solution, combined with the efficient transport of Y (III) across the membrane, are noteworthy findings. Donnan dialysis emerges as a promising membrane separation process for the removal of Y(III) from multi-element solutions, showing potential for future applications in real- assays with AMD.

3.3. Y(III) removal by strain M. qingshengii J19

To evaluate the ability of strain J19 to remove Y(III) from the receiver solution, the Donnan dialysis process was combined with the addition of the selected strain to the receiver compartment. The process was divided into two distinct stages: 1) Y(III) transport from the multi-element feed solution to the receiver solution across the membrane (1st stage), and 2) Y(III) removal from the receiver solution using strain J19 (2nd stage). In the 2nd stage, the removal of Y(III) was achieved through Y cellular immobilization by strain J19. As demonstrated in our previous work, the removal of Y is primarily associated with the binding of phosphorous to the cell surface of strain J19, forming a Y-P biocrystal

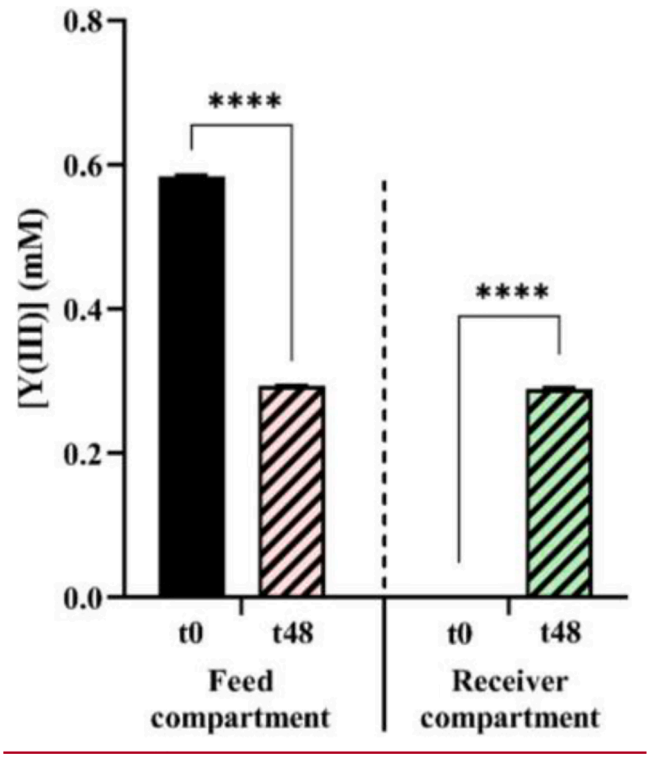

Fig. 5. Concentration of Y(III) measured in both receiver and feed solutions at t0 and t48 from the 1st stage assay, corresponding to the initial and 48 h of the assay, respectively.

[52]. Our published results showed that Y removal by J19 does not occur by biosorption, but needs cells metabolically active to enhance Y immobilization. The Y biomineralization process, involving the phosphate groups on the cell surface, was proposed as the bacterial strategy for Y immobilization. Given the extremely low pH, high salt concentration, and absence of nutrients in the receiver solution, the selected strain cannot grow under these conditions. Since the strain must be in its metabolically active growth phase to efficiently remove Y, it was necessary to carry out these two stages separately. In the 2nd stage, the receiver solution was first neutralized to a pH of around 7, and then the growth medium was introduced into the receiver compartment.

Fig. 5 shows that 49.4 ± 0.5 % of Y(III) was recovered in the receiver solution, indicating that half of Y(III) was efficiently transported from the multi-element feed solution to the receiver solution after 48 h of the assay, reaching an equilibrium of ions in both compartments. This result supports previous findings (Fig. 3), where at the same time point, 52.8 ± 0.35 % of Y(III) was also recovered. After 48 h of Y(III) transport, SEM-EDS analysis was performed to determine whether all Y^{3+} ions were completely transported across the membrane or if any were retained in it. The spatial distribution of Y across the membrane is shown in the EDS map in Fig. 6a, while Fig. 6b displays the EDS average spectrum, depicting the overall elemental composition detected in the membrane area. Analysis of the EDS spectrum did not detect Y in the CEM material. However, this does not exclude the potential for a small amount of Y to be retained in the membrane, as indicated in Fig. 6b. Even with the possibility of minimal Y fixation in the CEM material, it did not impact its recovery, validating that Y(III) was efficiently transported between compartments.

Once the 1st stage was completed, adjustments were made to the receiver solution, which contained approximately half of the initial concentration of Y(III) from the feed solution (0.4 mM). These adjustments included dilution by adding a new 2x concentrated growth medium and increasing the pH to optimize conditions for the growth of strain J19. At this point, the concentration of Y(III) in the receiver compartment was 4 times lower than the initial concentration in the feed solution. The Y(III) removal from the receiver solution during the growth of strain J19 was evaluated and is shown in Fig. 7a. Three incubation times were considered: t0 (the beginning of strain J19 growth), t24 (after 24 h of strain J19 growth) and t48 (after 48 h of strain J19 growth). During the 2nd stage assay, viable cell count evaluation revealed significantly higher CFUs at 24 h (t24) and 48 h (t48) compared to the initial growth time (t0) (Fig. S5), while strain J19 progressively removed Y(III) from the solution, achieving removal efficiencies of 38.3 ± 0.74 and 88.9 ± 3.68 % after 24 h and 48 h of growth, respectively. Furthermore, we showed that the strain J19 was able to immobilize high concentrations of Y in their cells, reaching values of 52.1 ± 0.45 and 61.5 ± 0.39 μg Y/mg protein after 24 h and 48 h of growth, respectively (Fig. 7b). That cellular growth is essential to attain an efficient Y immobilization by J19 cells as recently demonstrated [52]. The immobilization of Y was previously studied and reported as a biomineralization process achieved through Y adsorption to the phosphate groups present on the bacterial surface, resulting in Y(III) phosphate biocrystals [52]. Additionally, even in the presence of other cation metals in the receiver solution, the removal of Y(III) was not affected, nor was the capacity of Y cellular immobilization.

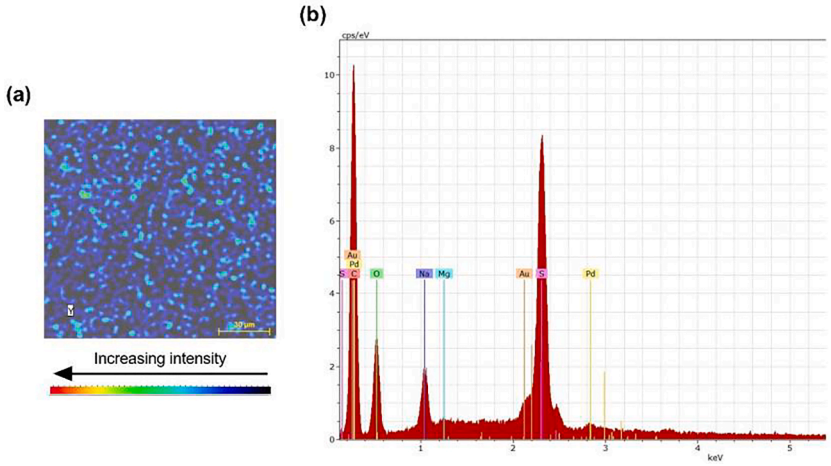

Fig. 6. Elemental composition of the membrane at the end of the 1st stage assay. EDS map shows the distribution of Y in the membrane **(a).** EDS average spectrum from the EDS map **(b)**. Means ± standard deviations – error bars – were calculated from two independent experiments. * indicates a significant difference from t0.

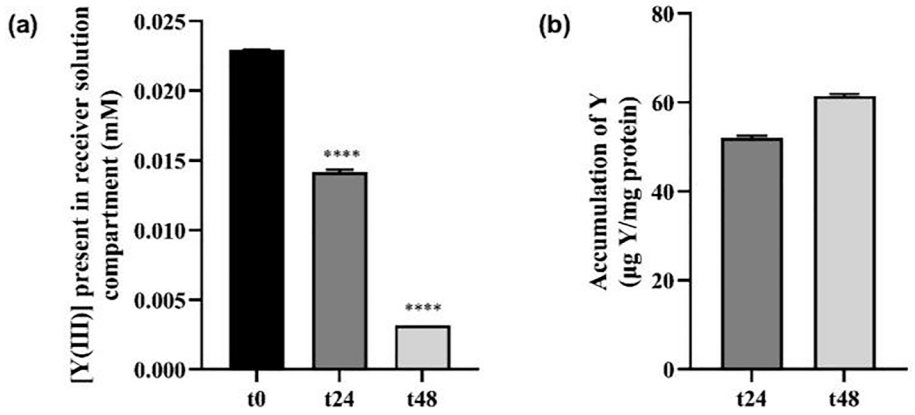

Fig. 7. Y(III) depletion from the receiver solution **(a)** and Y accumulation by strain J19 **(b)** over 48 h of growth from the 2nd stage experiment. The concentration of Y accumulated (considering both intracellular and surface-complexed parts of Y(III)) is shown after normalization for protein content. Means ± standard deviations – error bars – were calculated from two independent experiments. * indicates significant difference from t0.

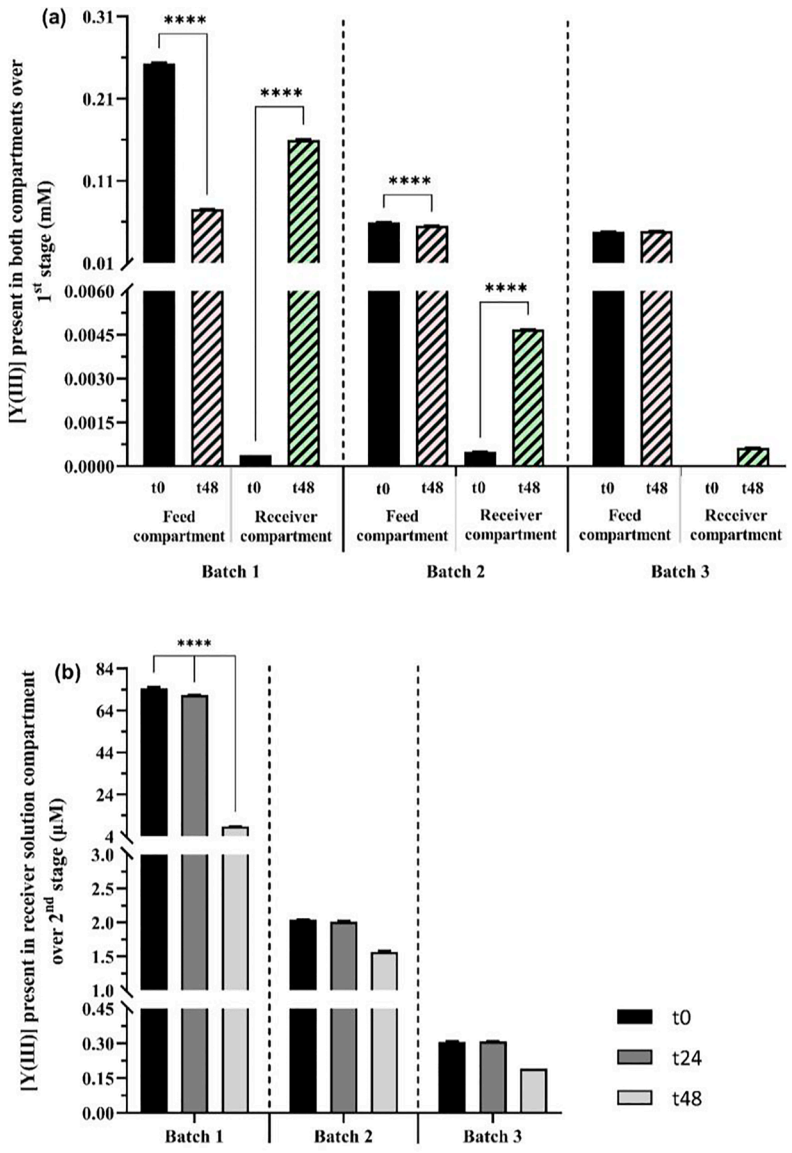

Fig. 8. Concentration of Y(III) measured in both receiver and feed solutions at t0 and t48 (1st stage) **(a)** and Y(III) depletion over 48 h of strain J19 growth (2nd stage) **(b)**, during the three batches. Means ± standard deviations – error bars – were calculated from two independent experiments. * indicates significant difference from t0, beginning of the experiment for each renewal solution time **(a)**, and t0, beginning of bacterial growth **(b)**.

The Y accumulation yields by strain J19 were 32.8 ± 0.29 and 60.3 ± 0.37 % for 24 h and 48 h of growth, respectively [Eq. (2)]. Despite the limited data available regarding the accumulation of REEs in cells, strain J19 was capable of a high removal of Y(III) present in the receiver solution, similar to the study carried out with strain *Thermus scotoductus* SA-01 when treated with europium (Eu) [56]. These results are remarkable given the lack of literature regarding the accumulation of REEs in cells, thus revealing the strain under study to be, for the first time, a very promising organism for removing Y(III) from multi-element solutions.

3.4. Evaluation of the capacity for repeated use of the membrane

This study was performed to assess the membrane's capacity for maximum removal of Y(III) in a repeated operation batch mode, maintaining the feed solution and renewing the receiver solution twice. The renewal of the receiver compartment solution was performed to transport the remaining Y(III) present in the feed compartment. Fig. 8a shows that Y(III) was efficiently transported to its maximum removal using the same membrane since the beginning of the assay, reaching recovery levels of 63.2 ± 0.11, 7.8 ± 0.03, and 1.3 ± 0.01 % of Y(III) during the three batches, respectively. In the assay where the 2nd stage was performed (Fig. 8b), strain J19 could remove Y(III) from the solution over time, reaching a significant removal of 88.3 ± 0.16 % of Y(III) after 48 h of bacterial growth over the first batch. However, since the amount of Y (III) in the last two batches was very low, the Y(III) removal in these two batches was not significant, despite showing removal values of 23.2 ± 0.82 and 38.2 ± 0.19 % of Y(III), respectively.

These results suggest that the membrane can be used successively until the maximum removal of Y(III) is reached. The only limitation of this assay is the initial amount of Y(III) present in the feed compartment. Therefore, if there is a continuous influx of metal in the respective compartment, it can be effectively removed.

4. Conclusions

This study provided a conceptual framework for understanding the equilibrium (i.e., between Y^{3+} in the solution and those interacting with the CEM) and kinetic (i.e., the rate at which Y^{3+} are removed or transported through the CEM) aspects of Y(III) removal through Donnan dialysis, involving a CEM with high Y(III) affinity. This system can successfully recover this metal from contaminated leachates, even when Y(III) is present at low concentrations within high concentrations of other metals. The primary conclusions of this work are:

- The Fumasep FKS-PEP-130 membrane was found to be suitable for the recovery of Y(III).
- Maximum Y(III) recovery was obtained with a high concentration of NaCl (0.5 M) and extremely low pH (0.8) in the receiver solution compartment, reaching a recovery of around 69 %.
- In multi-element feed solutions, the Y(III) recovery process was not affected by the presence of other cations.
- Y(III) was not retained on the membrane, being efficiently transported from one compartment to the other.
- The proposed approach with the addition of a biological treatment for Y(III) removal must be carried out in two sequential stages to adjust the conditions of the receiver solution to favor bacterial growth.
- The selected strain J19 efficiently removed Y(III) from the solution, reaching a maximum accumulation of approximately 61 μg Y/mg of protein, presenting an accumulation yield of around 61 % compared to the initial concentration of Y(III) present in the feed solution (0.4 mM).
- The membrane could be continuously used without affecting its Y(III) transport efficiency.

There are advantages to employing the proposed CEM transport/coupled biological treatment concept, which offers a promising and environmentally friendly alternative for recovering Y(III) from industrial mining solutions, such as AMD, compared to conventional bioremediation processes. Our proposed concept is advantageous for future assays using AMD, as it is the first optimized method that minimizes waste production while effectively separating metals from sulfates. This is achieved by using an IEM to separate cations from anions, particularly sulfates, which are present in higher concentrations, preventing unwanted releases into aquatic systems. Moreover, the concept allows for the selective removal of target metals with specific bacteria, thereby contributing to both environmental decontamination and sustainable metal recovery from multi-element solutions.

Future work will be necessary to define the best strategy to address the limitations of the 2nd stage, as the current approach of discarding half of the receiver solution and replacing it with a new medium. To optimize this stage and make the overall process more efficient and user-friendly, future research efforts must focus on addressing this issue. Additionally, further validation of the proposed concept with real-field AMD solutions is necessary to apply it as a tool for designing and scaling up the process. This can be easily achieved by using membrane contactors with larger membrane areas, making the process practical for industrial applications and ensuring a high level of environmental protection through the bioremediation process.

Declaration of competing interest

The authors declare that they have no known competing financial interests or personal relationships that could have appeared to influence the work reported in this paper.

Data availability

Data will be made available on request.

Acknowledgements

This work was supported by the projects Biorecover from the European Union's Horizon 2020 research and innovation program under grant agreement No 821096 and ERA-MIN 2 REVIVING ERA-MIN-2019_67 from the Fundação para a Ciência e Tecnologia (FCT) and sponsored by the FEDER funds through the program COMPETE – Programa Operacional Factores de Competividade – and by national funds through FCT, under projects UIDB/00285/2020 and LA/P/0112/2020. This work was also supported by the Associate Laboratory for Green Chemistry - LAQV which is financed by national funds from FCT/MCTES (UIDB/50006/2020 and UIDP/50006/2020.

Carina Coimbra was supported by POCH (cofunded by the European Social Fund and national funding by MCTES), through a PhD research grant (SFRH/BD/147292/2019) from FCT. Access to TAIL-UC analytical facilities is gratefully acknowledged.

Appendix A. Supplementary material

Supplementary data to this article can be found online at https://doi.org/10.1016/j.seppur.2024.129460.

References

[1] G. Morteani, The rare earths: their minerals, production and technical use, Eur. J. Mineral. 3 (1991) 641–650, https://doi.org/10.1127/ejm/3/4/0641.
[2] P. Möller, Rare earth mineral deposits and their industrial importance, lanthanides, Tantalum and Niobium (1989) 171–188, https://doi.org/10.1007/978-3-642-87262-4_6.
[3] M. Hermassi, M. Granados, C. Valderrama, N. Skoglund, C. Ayora, J.L. Cortina, Impact of functional group types in ion exchange resins on rare earth element recovery from treated acid mine waters, J. Clean. Prod. 379 (2022) 134742, https://doi.org/10.1016/j.jclepro.2022.134742.

[4] S.A. Cotton, Scandium, Yttrium & the Lanthanides: Inorganic & Coordination Chemistry, in: Encyclopedia of Inorganic Chemistry, John Wiley & Sons, Ltd, Chichester, UK, 2006. doi: 10.1002/0470862106.ia211.

[5] J.A. Cotruvo, The chemistry of lanthanides in biology: recent discoveries, emerging principles, and technological applications, ACS Cent Sci 5 (2019) 1496–1506, https://doi.org/10.1021/acscentsci.9b00642.

[6] European Commission, Study on the Critical Raw Materials for the EU 2023 - Final Report, 2023. doi: 10.2873/725585.

[7] R. León, F. Macías, C.R. Cánovas, R. Millán-Becerro, R. Pérez-López, C. Ayora, J. M. Nieto, Evidence of rare earth elements origin in acid mine drainage from the Iberian Pyrite Belt (SW Spain), Ore Geol. Rev. 154 (2023) 105336, https://doi.org/10.1016/j.oregeorev.2023.105336.

[8] A. Lozano, A. Fernández-Martínez, C. Ayora, D. Di Tommaso, A. Poulain, M. Rovezzi, C. Marini, Solid and aqueous speciation of yttrium in passive remediation systems of acid mine drainage, Environ. Sci. Tech. 53 (2019) 11153–11161, https://doi.org/10.1021/acs.est.9b01795.

[9] C. Ayora, F. Macías, E. Torres, A. Lozano, S. Carrero, J.-M. Nieto, R. Pérez-López, A. Fernández-Martínez, H. Castillo-Michel, Recovery of rare earth elements and yttrium from passive-remediation systems of acid mine drainage, Environ. Sci. Tech. 50 (2016) 8255–8262, https://doi.org/10.1021/acs.est.6b02084.

[10] M. Hermassi, M. Granados, C. Valderrama, C. Ayora, J.L. Cortina, Recovery of rare earth elements from acidic mine waters: an unknown secondary resource, Sci. Total Environ. 810 (2022) 152258, https://doi.org/10.1016/j.scitotenv.2021.152258.

[11] L. Echeverry-Vargas, L.M. Ocampo-Carmona, Recovery of rare earth elements from mining tailings: a case study for generating wealth from waste, Minerals 12 (2022) 948, https://doi.org/10.3390/min12080948.

[12] F. Xie, T.A. Zhang, D. Dreisinger, F. Doyle, A critical review on solvent extraction of rare earths from aqueous solutions, Miner. Eng. 56 (2014) 10–28, https://doi.org/10.1016/j.mineng.2013.10.021.

[13] D. Shin, J. Kim, B. Kim, J. Jeong, J. Lee, Use of phosphate solubilizing bacteria to leach rare earth elements from monazite-bearing ore, Minerals 5 (2015) 189–202, https://doi.org/10.3390/min5020189.

[14] H. Al-Zoubi, A. Rieger, P. Steinberger, W. Pelz, R. Haseneder, G. Härtel, Optimization study for treatment of acid mine drainage using membrane technology, Sep. Sci. Technol. 45 (2010) 2004–2016, https://doi.org/10.1080/01496395.2010.480963.

[15] Y.W. Siew, K.L. Zedda, S. Velizarov, Nanofiltration of simulated acid mine drainage: effect of pH and membrane charge, Appl. Sci. 10 (2020) 400, https://doi.org/10.3390/app10010400.

[16] I.L.R. Wallrich, B.W. Stewart, R.C. Capo, B.C. Hedin, T.T. Phan, Neodymium isotopes track sources of rare earth elements in acidic mine waters, Geochim. Cosmochim. Acta 269 (2020) 465–483, https://doi.org/10.1016/j.gca.2019.10.044.

[17] A. Roa, J. López, J.L. Cortina, Recovery of rare earth elements from acidic mine waters: a circular treatment scheme utilizing selective precipitation and ion exchange, Sep. Purif. Technol. 338 (2024), https://doi.org/10.1016/j.seppur.2024.126525.

[18] L.B. José, A.C.Q. Ladeira, Recovery and separation of rare earth elements from an acid mine drainage-like solution using a strong acid resin, J. Water Process Eng. 41 (2021), https://doi.org/10.1016/j.jwpe.2021.102052.

[19] J. Gómez, H. Giraldo, G. Piaggio, L. Barros, M. Quilaqueo, Y.M. Quintero, A. García, S. Santoro, E. Curcio, H. Estay, Recovery of copper sulfate from acidic mine waters by membrane crystallization, J Memb Sci 700 (2024), https://doi.org/10.1016/j.memsci.2024.122707.

[20] K. Menzel, L. Barros, A. García, R. Ruby-Figueroa, H. Estay, Metal sulfide precipitation coupled with membrane filtration process for recovering copper from acid mine drainage, Sep. Purif. Technol. 270 (2021), https://doi.org/10.1016/j.seppur.2021.118721.

[21] X. Zhang, L. Zeng, Y. Wang, J. Tian, J. Wang, W. Sun, H. Han, Y. Yang, Selective separation of metals from wastewater using sulfide precipitation: a critical review in agents, operational factors and particle aggregation, J. Environ. Manage. 344 (2023), https://doi.org/10.1016/j.jenvman.2023.118462.

[22] A. Breytus, D. Hasson, R. Semiat, H. Shemer, Ion exchange membrane adsorption in Donnan dialysis, Sep. Purif. Technol. 226 (2019) 252–258, https://doi.org/10.1016/j.seppur.2019.05.084.

[23] H. Chen, M. Rose, M. Fleming, S. Souizi, U. Shashvatt, L. Blaney, Recent advances in Donnan dialysis processes for water/wastewater treatment and resource recovery: a critical review, Chem. Eng. J. 455 (2023) 140522, https://doi.org/10.1016/j.cej.2022.140522.

[24] B. Zhao, H. Zhao, J. Ni, Arsenate removal by donnan dialysis: effects of the accompanying components, Sep. Purif. Technol. 72 (2010) 250–255, https://doi.org/10.1016/j.seppur.2010.02.013.

[25] T.A. Davis, DONNAN DIALYSIS, in: Encyclopedia of Separation Science, Academic Press, 2000: pp. 1701–1707.

[26] K.S. Barros, M. Carvalheira, B.C. Marreiros, M.A.M. Reis, J.G. Crespo, V. Pérez-Herranz, S. Velizarov, Donnan dialysis for recovering ammonium from fermentation solutions rich in volatile fatty acids, Membranes (basel) 13 (2023) 347, https://doi.org/10.3390/membranes13030347.

[27] S. Velizarov, Transport of arsenate through anion-exchange membranes in Donnan dialysis, J Memb Sci 425–426 (2013) 243–250, https://doi.org/10.1016/j.memsci.2012.09.012.

[28] M. Pessoa-Lopes, J.G. Crespo, S. Velizarov, Arsenate removal from sulphate-containing water streams by an ion-exchange membrane process, Sep. Purif. Technol. 166 (2016) 125–134, https://doi.org/10.1016/j.seppur.2016.04.032.

[29] I. Marzouk, L. Dammak, L. Chaabane, B. Hamrouni, Optimization of chromium (Vi) removal by donnan dialysis, Am. J. Analyt. Chem. 04 (2013) 306–313, https://doi.org/10.4236/ajac.2013.46039.

[30] U. Shashvatt, F. Amurrio, C. Portner, L. Blaney, Phosphorus recovery by donnan dialysis: membrane selectivity, diffusion coefficients, and speciation effects, Chem. Eng. J. 419 (2021) 129626, https://doi.org/10.1016/j.cej.2021.129626.

[31] A. Beck, M. Ernst, Kinetic modeling and selectivity of anion exchange in Donnan dialysis, J. Membr. Sc.i 479 (2015) 132–140, https://doi.org/10.1016/j.memsci.2014.12.037.

[32] C. Agarwal, R.W. Cattrall, S.D. Kolev, Donnan dialysis based separation of gold(III) from electronic waste solutions using an anion exchange pore-filled membrane, J. Memb. Sci. 514 (2016) 210–216, https://doi.org/10.1016/j.memsci.2016.04.033.

[33] H. Takahashi, K. Kikuchi, T. Sugawara, Ion-exchange equilibrium and diffusion of yttrium and lanthanum in a cation-exchange membrane, Kagaku Kogaku Ronbunshu 19 (1993) 99–105, https://doi.org/10.1252/kakoronbunshu.19.99.

[34] S. Velizarov, J. Crespo, Water treatment using the new concept of ion exchange membrane bioreactor, Pol. J. Chem. Technol. 5 (2003) 40–43. https://www.researchgate.net/publication/235752064.

[35] S. Velizarov, J.G. Crespo, M.A. Reis, Removal of nitrate from water in a novel ion exchange membrane bioreactor, Water Sci Technol Water Supply 2 (2002) 161–167, https://doi.org/10.2166/ws.2002.0059.

[36] C.T. Matos, A.M. Sequeira, S. Velizarov, J.G. Crespo, M.A.M. Reis, Nitrate removal in a closed marine system through the ion exchange membrane bioreactor, J. Hazard. Mater. 166 (2009) 428–434, https://doi.org/10.1016/j.jhazmat.2008.11.038.

[37] A. Oehmen, R. Viegas, S. Velizarov, M.A.M. Reis, J.G. Crespo, Removal of heavy metals from drinking water supplies through the ion exchange membrane bioreactor, Desalination 199 (2006) 405–407, https://doi.org/10.1016/j.desal.2006.03.091.

[38] C. Filote, M. Roşca, R. Hlihor, P. Cozma, I. Simion, M. Apostol, M. Gavrilescu, Sustainable application of biosorption and bioaccumulation of persistent pollutants in wastewater treatment: current practice, Processes 9 (2021) 1696, https://doi.org/10.3390/pr9101696.

[39] V. Guiné, L. Spadini, G. Sarret, M. Muris, C. Delolme, J.-P. Gaudet, J.M.F. Martins, Zn sorption to three gram- bacteria_combined titration, modeling, and EXAFS study, Environ. Sci. Tech. 40 (2006) 1806–1813.

[40] E.S. Kazak, E.G. Kalitina, N.A. Kharitonova, G.A. Chelnokov, E.V. Elovskii, I. V. Bragin, Biosorption of rare-earth elements and yttrium by heterotrophic bacteria in an aqueous environment, Mosc. Univ. Geol. Bull. 73 (2018) 287–294, https://doi.org/10.3103/S0145875218030043.

[41] S.A. Razzak, M.O. Faruque, Z. Alsheikh, L. Alsheikhmohamad, D. Alkuroud, A. Alfayez, S.M.Z. Hossain, M.M. Hossain, A comprehensive review on conventional and biological-driven heavy metals removal from industrial wastewater, Environ. Adv. 7 (2022) 100168, https://doi.org/10.1016/j.envadv.2022.100168.

[42] Y. Takahashi, X. Châtellier, K.H. Hattori, K. Kato, D. Fortin, Adsorption of rare earth elements onto bacterial cell walls and its implication for REE sorption onto natural microbial mats, Chem. Geol. 219 (2005) 53–67, https://doi.org/10.1016/j.chemgeo.2005.02.009.

[43] X. Pan, W. Wu, J. Lü, Z. Chen, L. Li, W. Rao, X. Guan, Biosorption and extraction of europium by Bacillus thuringiensis strain, Inorg. Chem. Commun. 75 (2017) 21–24, https://doi.org/10.1016/j.inoche.2016.11.012.

[44] P. Dhanwal, A. Kumar, S. Dudeja, H. Badgujar, R. Chauhan, A. Kumar, P. Dhull, V. Chhokar, V. Beniwal, Biosorption of heavy metals from aqueous solution by bacteria isolated from contaminated soil, Water Environ. Res 90 (2018) 424–430, https://doi.org/10.2175/106143017X15131012152979.

[45] L.M. Coelho, H.C. Rezende, L.M. Coelho, P.A.R. de Sousa, D.F.O. Melo, N.M.M. Coelho, Bioremediation of Polluted Waters Using Microorganisms, in: Advances in Bioremediation of Wastewater and Polluted Soil, InTech, 2015. doi: 10.5772/60770.

[46] J. Jung, A. Blüher, M. Lakatos, G. Cuniberti, Metal ion binding and tolerance of bacteria cells in view of sensor applications, J. Sens. Sens. Syst. 7 (2018) 433–441, https://doi.org/10.5194/jsss-7-433-2018.

[47] L. Zhou, F. Dong, W. Zhang, Y. Chen, L. Zhou, F. Zheng, Z. Lv, J. Xue, D. He, Biosorption and biomineralization of U(VI) by *Kocuria rosea*: involvement of phosphorus and formation of U-P minerals, Chemosphere 288 (2022), https://doi.org/10.1016/j.chemosphere.2021.132659.

[48] Z. Chen, X. Pan, H. Chen, X. Guan, Z. Lin, Biomineralization of Pb(II) into Pb-hydroxyapatite induced by *Bacillus cereus* 12–2 isolated from lead–zinc mine tailings, J. Hazard. Mater. 301 (2016) 531–537, https://doi.org/10.1016/j.jhazmat.2015.09.023.

[49] Y. Jiang, X. Zhao, Y. Zhou, C. Ding, Effect of the phosphate solubilization and mineralization synergistic mechanism of *Ochrobactrum* sp. on the remediation of lead, Environ. Sci. Pollut. Res. 29 (2022) 58037–58052, https://doi.org/10.1007/s11356-022-19960-y.

[50] C. Coimbra, R. Branco, P.V. Morais, Efficient bioaccumulation of tungsten by *Escherichia coli* cells expressing the *Sulfitobacter dubius* TupBCA system, Syst. Appl. Microbiol. 42 (2019), https://doi.org/10.1016/j.syapm.2019.126001.

[51] M.M. Bradford, A Rapid and sensitive method for the quantification of microgram quantities of protein utilizing the principle of protein-dye binding, Anal. Biochem. 72 (1976) 248–254.

[52] C. Coimbra, R. Branco, P.S.P. da Silva, J.A. Paixão, J.M.F. Martins, L. Spadini, P. V. Morais, Yttrium immobilization through biomineralization with phosphate by the resistant strain *Mesorhizobium qingshengii* J19, J. Appl. Microbiol. (2024), https://doi.org/10.1093/jambio/lxae156.

[53] Z. Hubicki, D. Koodynsk, Selective removal of heavy metal ions from waters and waste waters using ion exchange methods, in: Ion Exchange Technologies, InTech, 2012. doi: 10.5772/51040.
[54] N.H.B. Mohammed, W.Z.W. Yaacob, Remediation of AMD using industrial waste adsorbents, AIP Conference Proceedings (2016) 0600431–0600437, https://doi.org/10.1063/1.4966881.
[55] J.A. Torres-Martínez, A. Mora, P.S.K. Knappett, N. Ornelas-Soto, J. Mahlknecht, Tracking nitrate and sulfate sources in groundwater of an urbanized valley using a multi-tracer approach combined with a Bayesian isotope mixing model, Water Res. 182 (2020), https://doi.org/10.1016/j.watres.2020.115962.
[56] M. Maleke, A. Valverde, J.-G. Vermeulen, E. Cason, A. Gomez-Arias, K. Moloantoa, L. Coetsee-Hugo, H. Swart, E. van Heerden, J. Castillo, Biomineralization and bioaccumulation of europium by a thermophilic metal resistant bacterium, Front. Microbiol. 10 (2019) 1–10, https://doi.org/10.3389/fmicb.2019.00081.